

## STUDY OF LOCAL TURBULENT WIND CHARACTERISTICS AND WIND VELOCITY SIMULATIONS

RÓBERT ŠOLTÝS, MICHAL TOMKO AND STANISLAV KMEŤ

Results of the analyses of in situ measured wind records with a sampling frequency of 20 Hz and with the duration of 1 year are presented in the paper. Wind speed records were measured at Bily Kriz station in Beskydy by the Institute of Systems Biology and Ecology at the Academy of Sciences of the Czech Republic. Because a high measurement frequency for research applications was needed, wind velocity was measured according to the propagation speed of ultrasound signals. Records were performed by a GILL R3-100 ultrasonic anemometer positioned 18 m above the height of the terrain (approximately 5 m above the pine trees). From the annual record of wind velocities the measurement with the duration of 17.5 h was selected for further statistical processing. This measurement consists of 35 records of 30 min intervals. For selected data set statistical characteristics and power spectral density functions of the measured wind velocity components in the longitudinal, lateral and vertical direction are calculated. On the basis of the experimentally measured records of turbulent wind velocities the simulations of the wind field histories in the individual directions were generated using the Shinozuka method and developed WindSimul program. The evaluation of their statistical and frequency properties was performed. The physical importance of the mathematical approach and the functionality of the developed program were demonstrated and proved.

Obtained statistical and frequency properties of the longitudinal, lateral and vertical component of the measured turbulent wind can find a wider use in the dynamic analysis and design of structures in similar areas.

**Keywords:** turbulent wind, fluctuating velocity components, in situ measurement, statistical characteristics, frequency characteristics, power spectral density functions, wind velocity simulation

### 1. Introduction

The ever-increasing spans and heights of modern slender engineering structures result in the increasing significance of wind effects.

To include nonlinearities of both structural and aerodynamic origins, a time-domain analysis for the prediction of the maximum dynamic response of strongly nonlinear structures subjected to wind loads is recommended (Chen et al., 2000). Time-domain approaches require the generation of input wind histories of multi-dimensional wind fields which can be simulated numerically. Wind records have shown that wind velocity can be considered as a stationary multi-dimensional

and multi-variate random process. Consequently, the fluctuating component of the wind can be quantified by statistical functions whose spatial-temporal properties in the frequency domain are expressed by power spectral density functions.

Large numbers of papers which deal with such problems have been published over the last decades and significant progress has been made in the simulation of wind effects and in the prediction of the dynamic behaviour of light-weight structures. One of the reason of wind-induced vibrations of slender bridges are wind turbulence forces which have a considerable power (Tesar et al., 2008). It is recognized that the application of different turbulence models of wind often provides different evaluations for the dynamic response of the structure (Solari and Piccardo, 2001, Holmes, 2001). Kareem (2008) summarized a historical perspective, recent developments and future challenges in the probabilistic numerical simulation of wind effects. Some authors present the results of measurements in situ or wind tunnel tests while others investigate the problem in general terms theoretically, compare various models and data or study specific aspects through numerical experiments (Li et al., 2009). Lazzari et al. (2001) studied the modelling and simulation of wind velocity by considering a stationary, multivariate stochastic process, according to its prescribed cross-spectral density matrix. Naprstek (2001) investigated the stochastic stability of movement influenced by parametric noise which is generated by the interaction of a moving bluff body and an air flow. Hanzlik et al. (2005) presented the methodology for estimating wind effects based on a database-assisted design approach. Fu et al. (2007) developed two artificial neural network approaches (a backpropagation neural network and a fuzzy neural network) for the prediction of mean, root-mean-square pressure coefficients and time series of wind-induced pressures acting on a large roof structure. Carassale and Solari (2002) developed an analytic expression of the proper orthogonal decomposition for a class of processes, which include models usually adopted to represent atmospheric turbulence.

Analyses of in situ measured wind records and generation of numerical simulations of wind velocity histories are presented in this paper.

## **2. Measurements of wind velocities in situ**

Wind speed records were measured at Bily Kriz station in Beskydy by the Institute of Systems Biology and Ecology at the Academy of Sciences of the Czech Republic. Because a high recording frequency for research applications was needed, wind velocity was measured according to the propagation speed of ultrasound signals. Records were performed by a GILL R3-100 ultrasonic anemometer, which is part of a system for measuring the exchange of substances between the bark pocket and atmosphere. A view of the mast with the attached anemometer is shown in Figure 1. The sampling frequency was 20 Hz and the duration of records was 1 year. The records comprised all three components of wind velocity i.e. in the longitudinal, lateral and vertical direction. The device was positioned 18 m above the height of the terrain (approximately 5 m above the pine trees) as it is shown in Figure 1.

From the annual record of wind velocities the measurement performed in December 2010 (22.12.2010) with the duration of 17.5 h (1 050 min or 63 000 s) was selected for further statistical processing. This measurement consists of 35 records of 30 min intervals. The criterion for selecting the chosen intervals preferably required the highest mean wind velocity for an entire interval; approximately the same mean speeds and flow directions of a longitudinal component of the wind during individual 30 min time periods.



Figure 1. View of the mast with attached anemometer located on the mast at a height  $z = 18$  m

### 3. Statistical properties of the measured turbulent wind data

Fluctuating velocity components of wind were quantified by statistical functions. The velocity of the wind is considered to consist of a mean wind velocity component and a fluctuating velocity component due to the turbulence or gusting caused by the ground's roughness. The wind velocity components  $u(z, x, t)$ ,  $v(z, y, t)$ , and  $w(z, z, t)$  can be expressed as the sum of the mean wind velocity components  $\bar{u}(z, x)$ ,  $\bar{v}(z, y)$  and  $\bar{w}(z, z)$ , and, the fluctuating time-dependent velocity components  $u'(z, x, t)$ ,  $v'(z, y, t)$  and  $w'(z, z, t)$  in the form

$$\begin{Bmatrix} u(z, x, t) \\ v(z, y, t) \\ w(z, z, t) \end{Bmatrix} = \begin{Bmatrix} \bar{u}(z, x) \\ \bar{v}(z, y) \\ \bar{w}(z, z) \end{Bmatrix} + \begin{Bmatrix} u'(z, x, t) \\ v'(z, y, t) \\ w'(z, z, t) \end{Bmatrix} \quad (1)$$

where  $x$  represents the longitudinal direction (the along-wind direction),  $y$  is the lateral direction (the horizontal cross-wind direction) and  $z$  is the vertical direction (the vertical cross-wind direction) at height  $z$ .

The mean wind velocity is defined as

$$\bar{u} = \frac{1}{T} \int_0^T u(t) dt \quad (2)$$

and the standard deviation  $\sigma_u$  for the longitudinal direction is

$$\sigma_u = \sqrt{\sigma_u^2} = \sqrt{\frac{1}{T} \int_0^T (u(t) - \bar{u})^2 dt} \quad (3)$$

where  $\sigma^2$  is the variance of the wind velocity component and  $T$  is the integration time. Turbulence intensities in the longitudinal, lateral and vertical direction are calculated as

$$I_u = \frac{\sigma_u}{\bar{u}} 100\%, \quad I_v = \frac{\sigma_v}{\bar{u}} 100\%, \quad I_w = \frac{\sigma_w}{\bar{u}} 100\% \quad (4)$$

For further analyses two shorter records of wind velocity components in the longitudinal, lateral and vertical direction with duration of 30 min and 60 s were randomly selected from the experimentally measured 17.5 h record of wind velocity data.

Statistical characteristics for the longitudinal, lateral and vertical component of the measured wind velocities obtained from the record with duration of 17.5 h, 30 min and 60 s are presented in Table 1, 2 and 3.

Table 1. Statistical characteristics of the measured wind velocity component in the longitudinal direction  $u(z, x, t)$  obtained from the record with duration of 17.5 h, 30 min and 60 s and 60 s simulation

Statistical properties		Record	Record	Record	Simulation S1
		(17.5 h)	(30 min)	(60 s)	(60 s)
$u_{min}$	$(ms^{-1})$	-3.9412	-3.9412	1.7837	2.7043
$\bar{u}$	$(ms^{-1})$	6.7988	8.83	9.5945	9.5981
$u_{max}$	$(ms^{-1})$	20.6931	16.8189	16.1748	16.7828
$\sigma_u$	$(ms^{-1})$	2.2409	2.3507	2.7872	2.4725
$I_u$	(%)	32.96	26.62	29.05	25.7696

Table 2. Statistical characteristics of the measured wind velocity component in the lateral direction  $v(z, y, t)$  obtained from the record with duration of 17.5 h, 30 min and 60 s and 60 s simulation

Statistical properties		Record	Record	Record	Simulation S1
		(17.5 h)	(30 min)	(60 s)	(60 s)
$v_{min}$	$(ms^{-1})$	-12.1888	-10.9679	-5.38	-6.4954
$v$	$(ms^{-1})$	0.4462	-0.9125	-0.0144	-0.013
$v_{max}$	$(ms^{-1})$	9.8004	9.2338	5.8121	6.1939
$\sigma_v$	$(ms^{-1})$	1.9285	2.0579	2.1431	2.4246
$I_v$	(%)	23.14	23.31	22.34	25.2711

Table 3. Statistical characteristics of the measured wind velocity component in the vertical direction  $w(z, z, t)$  obtained from the record with duration of 17.5 h, 30 min and 60 s and 60 s simulation

Statistical properties		Record	Record	Record	Simulation S1
		(17.5 h)	(30 min)	(60 s)	(60 s)
$w_{min}$	$(ms^{-1})$	-6.7436	-4.1477	-2.1691	-2.1353
$w$	$(ms^{-1})$	1.5353	2.0497	2.1245	2.1237
$w_{max}$	$(ms^{-1})$	9.9584	8.9152	6.5567	6.8957
$\sigma_w$	$(ms^{-1})$	1.0879	1.2215	1.1756	1.4907
$I_w$	(%)	16	13.83	12.25	15.5369

Time course of the experimentally measured longitudinal wind flow direction with duration of 17.5 h is shown in Figure 2. Rosette of the relative rate of the occurrence of a longitudinal wind flow direction obtained from the measurement with duration of 17.5 h is shown in Figure 3. Figure 3 gives a succinct view of how a wind flow direction was distributed at this particular location. Courses of the mean wind velocities ( $\bar{u}$ ,  $\bar{v}$  and  $\bar{w}$ ) and variances of wind velocities ( $\sigma_u^2$ ,  $\sigma_v^2$  and  $\sigma_w^2$ ) in the longitudinal, transversal and vertical direction calculated from 35 measured records with duration of 30 min are shown in Figure 4 and 5.

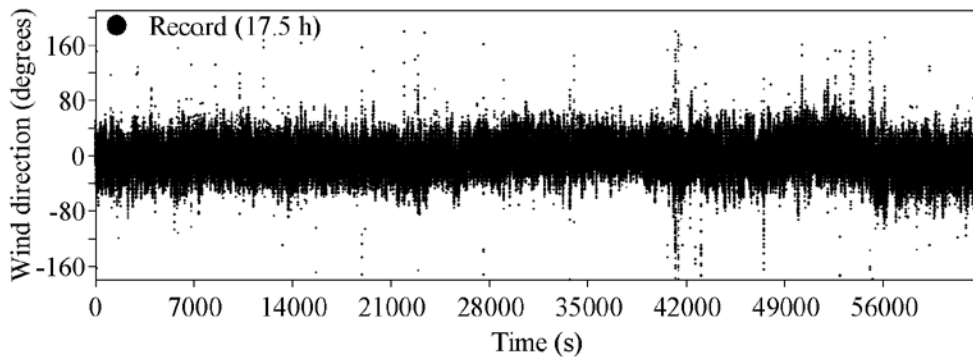


Figure 2. Time course of the experimentally measured longitudinal wind flow direction with duration of 17.5 h is shown

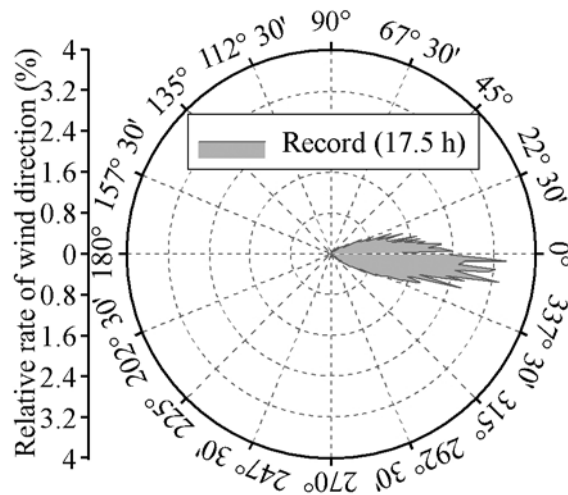


Figure 3. Rosette of the relative rate of the occurrence of a longitudinal wind flow direction obtained from the measurement with duration of 17.5 h

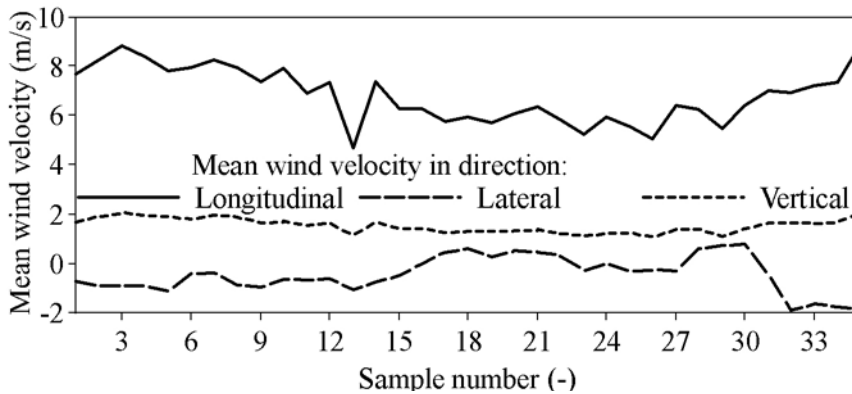


Figure 4. Courses of mean wind velocities ( $\bar{u}$ ,  $\bar{v}$  and  $\bar{w}$ ) in the longitudinal, lateral and vertical direction calculated from 35 measured records with a duration of 30 min

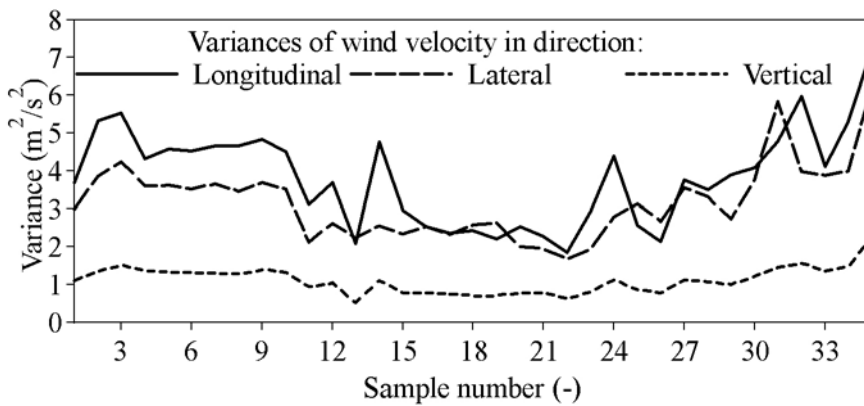


Figure 5. Courses of variances of wind velocities ( $\sigma_u^2$ ,  $\sigma_v^2$  and  $\sigma_w^2$ ) in the longitudinal, lateral and vertical direction calculated from 35 measured records with duration of 30 min

If the duration of the record increases the mean wind velocity in the longitudinal direction decreases as it is shown in Table 1 (Fischer et al., 1977). In longer records, larger extreme values of minimum and maximum wind velocities occur.

#### 4. Spectral properties of the measured wind velocities

The wind power spectrum statistically represents the energy distribution in a turbulent flow field, which can be viewed as a superposition of eddies ranging spatially from millimeters to kilometers and temporally from a fraction of a second to hours. The behaviour of turbulence spectrum within the atmospheric boundary layer follows the Kolmogorov hypotheses in the inertial sub-range, which ensures spectral description to have a universal shape when scaled appropriately in a certain range of frequencies or wave-numbers (Li et al., 2012).

To be able to simulate realistic behaviour of structures and reliably predict their response a suitable spatial wind model is necessary. For a generation of such wind models the power spectral density functions in the longitudinal, lateral and vertical direction are required.

##### 4.1 Spectral turbulence model of an atmospheric boundary layer – theoretical background

One of the critical features of the atmospheric turbulence in the definition of structural loads is the spectral description of wind velocity fluctuations (Li et al., 2012).

In the neutral atmospheric stratification (Panofsky and Dutton, 1984), the turbulence energy spectrum can be rewritten as

$$\frac{nS_u(z, n)}{u_*^2} = A_u f^{-2/3} \quad (5)$$

where  $A_u$  is a non-dimensional parameter and typically equals to 0.27 (Yu et al., 2008), and  $f$  is the Monin coordinate, defined as  $f = nz / \bar{u}$  herein, (Li et al., 2012).

Measurements suggested that for engineering applications Eq. 5 provides a good estimate of the power spectrum in the high frequency range ( $f > 0.2$ ), (Frichl and McVehil, 1970; Simiu, 1974). The following expression for wind power spectra has accordingly been advanced (Olesen et al., 1984)

$$\frac{nS_u(z, n)}{u_*^2} = \frac{AR^2 f^\gamma}{(C + Bf^\alpha)^\beta} \quad (6)$$

where  $f = n\Lambda / \bar{u}$ ,  $\Lambda$  is a length scale, which can be chosen as the height  $z$  above ground or the longitudinal integral scale  $L_u^x$  at height  $z$  or a constant length over entire height;  $A$ ,  $B$ ,  $C$ ,  $\alpha$ ,  $\beta$  and  $\gamma$  are six parameters,  $R$  is the ratio between the standard deviation of the turbulence components and the friction velocity, which is akin to turbulence intensity and it has been referred to as turbulence ratio in Masters et al. (2010)

$$R = \frac{\sigma_u}{u_*} \quad (7)$$

Each parameter in the universal model (Eq. 6) would have its own influence on the energy distribution and physical meaning which was investigated by Li et al., 2012).

Based on theoretical consideration, spectral models represented by Eq. 6 should meet the following requirements (e.g. Kareem, 1985a, 1985b; Tieleman, 1995; Simiu and Scanlan, 1996; Tamura et al., 2001):

- the spectral slope in the inertial sub-range must be considered with Eq. 5, which leads to

$$\alpha\beta - \gamma = 2/3 \quad (8)$$

- when the frequency  $n$  approaches zero, the wind power spectrum should satisfy the following condition

$$S_u(0) = 4\sigma_u^2 \frac{L_u^x}{u} \quad (9)$$

- the derivative of  $S_u(n)$  which respects to  $n$  tends to 0 as  $n$  approaches 0

$$\frac{dS_u(n)}{dn} \rightarrow 0 \Big|_{n \rightarrow 0} \quad (10)$$

This requirement leads to  $\alpha \geq 1$ .

Accordingly, the universal wind power spectra model (Eq. 6) can be theoretically simplified in terms of the following four-parameter equation

$$\frac{nS_u(z, n)}{u_*^2} = \frac{AR^2 f}{(C + Bf^\alpha)^{5/3\alpha}} \quad (11)$$

where the parameter  $A$  mainly adjusts the total energy contained in the spectrum which equals to the variance of the fluctuating velocity; the parameter  $B$  controls the high frequency,  $C$  primarily governs the low frequency part and  $\alpha$  regulates the spectral shape to fit a „blunt“ or a „pointed“ model.

#### 4.2 Resultant power spectral density functions of the measured wind velocities

In order to investigate the frequency characteristics of the wind velocity, the power spectral density functions (PSD) for the wind velocity components were calculated using FlexPro software (FlexPro, 2005). The discrete Fourier transformation was used to transfer the time domain into the frequency domain representation. The power spectral density functions were determined using the fast Fourier transformation. Jang and Lee, 1998 adopted in their study the unit time length of 20 minutes for each data set (run, sample), and it was still adequate. They recommended that the recorded time per data might extend to 30 minutes for better results. Shiau and Chen (2002) used for the calculation of PSD 17 records with duration of 10 minutes and results compared with the von Kármán's form of spectrum equation. In our study 30 minutes lengths of each data set were used.

For each of the 35 measured records with 30 min durations, power spectral density functions and their average values were calculated for each discrete frequency, separately for the longitudinal, lateral and vertical component of wind. The average value of PSD is calculated as

$$\frac{n \cdot S_{aver}(n)}{u_*^2} = \frac{\sum_{i=1}^K \frac{n \cdot S(n,i)}{u_{*i}^2}}{K} \quad (12)$$

where  $u_{*i}$  is the friction velocity expressed as

$$u_{*i} = \frac{\bar{u}_i \cdot k}{\ln(z/z_0)} = \sigma_{u,i} \cdot k \quad (13)$$

and  $k$  is the von Kármán's constant ( $k \approx 0.4$ ).

PSD values have been smoothed in the frequency domain using the Hanning window defined as

$$w(n) = \cos^2\left(\frac{\pi n}{2a}\right), \text{ for } a = 2. \quad (14)$$

Mean values of power spectral densities were approximated by the following non-dimensional normalized power spectral density functions

- longitudinal direction

$$\frac{n \cdot S_u}{u_*^2} = \frac{297,2 \cdot f}{(1 + 73,127 \cdot f)^{5/3}} \quad (15)$$

- transversal direction

$$\frac{n \cdot S_v}{u_*^2} = \frac{250 \cdot f}{(1 + 65 \cdot f)^{5/3}} \quad (16)$$

- vertical direction

$$\frac{n \cdot S_w}{u_*^2} = \frac{9,137 \cdot f}{(1 + 38,331 \cdot f^{5/3})} \quad (17)$$

where  $f(z, n) = nz / \bar{u}(z)$  is a non-dimensional frequency determined by the frequency  $n$ , the height  $z$  above the terrain and by the mean wind velocity  $\bar{u}(z)$ ,  $u_*$  is the friction velocity and  $z_0 = 0,3$  m is the roughness length. For the investigated area with regular forest cover the height  $z$  above the terrain, representing the vertical distance from ground level to the position of the anemometer, is replaced with an effective height of  $z = 5.0$  m (Holmes, 2001). This represents the distance between the height of the anemometer and the top of the trees.

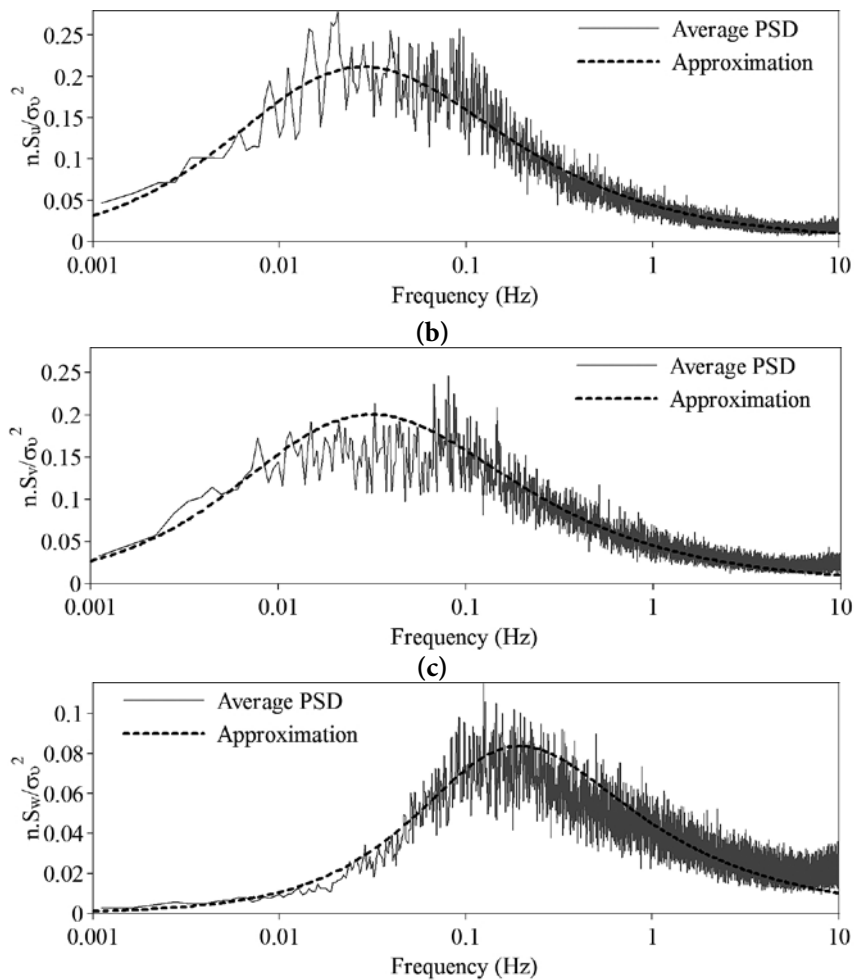


Figure 6. Normalized non-dimensional average power spectral density functions of wind velocities calculated from 35 measured records with duration of 30 min and their approximated functions in (a) the longitudinal, (b) transversal and (c) vertical direction

Normalized non-dimensional average power spectral density functions of wind velocities in the individual longitudinal, transversal and vertical direction calculated from 35 measured records with duration of 30 min and their approximated functions in the forms of Eq. (15), (16) and (17) are shown in Figure 6.

Courses of variances of wind velocities in the longitudinal and transversal direction calculated from 35 measured records with duration of 30 min are similar and their values are close to each other from both quantitative and qualitative aspects as it is shown in Figure 5. Consequently, power spectral density functions for the longitudinal and transversal direction also take values close to each other as it is clear from Figure 6a and 6b. Fluctuating energy of air flow in the longitudinal and transversal direction has mutually close values, which may be caused by local conditions (mountainous wooded terrain, orography, etc.).

### 4.3 Comparison of wind power spectral density formulations

In order to compare the frequency characteristics of the wind velocity components the approximated power spectral density functions calculated from expressions Eq. (15), (16) and (17) for the experimentally measured records were compared with those determined according to the analytical expressions proposed by several authors.

For illustration purposes, a comparison of the mean power spectral density function obtained from the measurement of the wind velocity component in the longitudinal, lateral and vertical direction with those obtained by the analytical expressions proposed by other authors are shown in Figure 7, 8 and 9. From the figures it can be seen, that global courses of individual power spectral density functions are similar and quantitative differences can be caused *e.g.* by the terrain's properties, orography and parameters for the site of measurement. The corresponding analytical expressions of the mean power spectral density functions of the wind velocity component in the longitudinal, lateral and vertical direction proposed by the various authors are presented in Table 4, 5 and 6. Davenport's formula (Eq. (19)) has been adopted by SNBCC (Supplement to the National Building Code of Canada, 1990) and ANSI (American National Standards Institute, 1990). It is noted that this spectrum has no relation with altitude. Harris's spectrum formula (Eq. (20)) has been adopted by ESDU (Engineering Science Unit, 1989) and it is not a function of altitude either. Kaimal and Simiu's spectrum formula (Eq. (22)) has been adopted by NBS (National Bureau of Standards, 1980). It can be applied to both low-frequency and high-frequency spectrum area (Jang and Lee, 1998). Expression proposed by Solari (Eq. (26)) is adopted in EN 1991-1-4, 2005. In the longitudinal direction is the power spectral density function proposed by the authors of this paper is the closest to the spectrum proposed by Solari, 1993 (Figure 7a). In the lateral direction is the power spectral density function proposed by the authors of this paper larger in a comparison with power spectral density functions proposed by other authors, which are caused by specific features of local natural conditions.

Table 4. Analytical expressions of the mean power spectral density functions of the wind velocity component in the longitudinal direction proposed by various authors

Author	Reference	$nS_u(z, n)/u^2$	Eq.
Davenport	Davenport, 1961	$4 x_1^2 / (1 + x_1^2)^{4/3}$	(19)
Harris	Harris, 1971	$4 x_1 / (1 + x_1^2)^{5/6}$	(20)
Hino	Hino, 1971	$0,475 k^2 x_2 / (1 + x_2)^{5/6}$	(21)
Kaimal & Simiu	Kaimal et al. 1972, Simiu, 1974	$200 f / (1 + 50f)^{5/3}$	(22)
Kareem	Kareem, 1985b	$335 f / (1 + 71f)^{5/3}$	(23)
Reinhold	Simiu & Scanlan, 1986	$4 (nL_u^x / \bar{u}) / (1 + 71.05(nL_u^x / \bar{u})^2)^{5/6}$	(24)
Solari	Solari, 1987	$2,21 \beta_u^{2,5} f / (1 + 3,31\beta_u^{1,5} f)^{5/3}$	(25)
Solari	Solari, 1993	$6,868 (fL_s/z) / [1 + 10,302(fL_{s/z})]^{5/3}$	(26)
Teunissen	Teunissen, 1980	$105 f / (0,4 + 3f)^{5/3}$	(27)
von Kármán	von Kármán, 1948	$4 (nL_u^x / \bar{u}) / (1 + 70.8(nL_u^x / \bar{u})^2)^{5/3}$	(28)

Note:  $x_1 = nL/\bar{u}_{10}$ ,  $L = 1200m$ ,  $\bar{u}_{10}$  is the mean velocity at the height of 10 m,  $x_2 = 250nz^{0.42}/\bar{u}$ ,  $\beta_u = \sigma_u^2/u^2 = 5.33$  is the factor of turbulence intensity and  $L_s = 300(z/200)^{(0.67+0.051nz_0)}$ , where  $z_0$  is the roughness length.

Table 5. Analytical expressions of the mean power spectral density functions of the wind velocity component in the lateral direction proposed by various authors

Author	Reference	$nS_u(z, n)/u^2_*$	Eq.
Kaimal	Kaimal et al., 1972	$17f/(1 + 9,5f)^{5/3}$	(29)
Simiu & Scanlan	Simiu & Scanlan, 1996	$15f/(1 + 9,5f)^{5/3}$	(30)
Teunissen	Teunissen, 1980	$17f/(0,38 + 9,5f)^{5/3}$	(31)

Table 6. Analytical expressions of the mean power spectral density functions of the wind velocity component in the vertical direction proposed by various authors

Author	Reference	$nS_u(z, n)/u^2_*$	Eq.
Busch & Panofsky	Holmes, 2001	$2,15 f/(1 + 11,6f^{5/3})$	(32)
Kaimal	Kaimal et al., 1972	$2f/(1+5,3f^{5/3})$	(33)
Panofsky & McCornick	Panofsky & McCornick, 1960	$6 f/(1 + 4f)^2$	(34)
Powell & Elderkin	Powell & Elderkin, 1974	$2,5 f/(1 + 5,47 f^{5/3})$	(35)
Simiu & Scanlan	Simiu & Scanlan, 1996	$3,36 f/(1 + 10 f^{5/3})$	(36)
Teunissen	Teunissen, 1980	$2 f 8(0,44 + 5,3f^{5/3})$	(37)

It is necessary to note, that in the standard EN 1991-1 - 4, 2005 power spectral density functions for the lateral and vertical direction of turbulent wind are not available. This standard contains only power spectral density functions for the longitudinal direction. That is why this study was done. For a detailed dynamic analysis of structures subjected to turbulent wind the spatial wind histories are required to obtain their realistic aero-elastic response and behaviour characteristics. For example, the most dynamic analyses of wind-excited stay or suspended cables are focused on the investigation of basic dynamically unstable phenomena and the modelling of aerodynamic forces acting on a cable which may be caused by: buffeting (from turbulence in the air flow), vortex shedding (from von Kármán vortices in the wake of the cable), galloping (self induction), wake galloping (fluid-elastic interaction of neighbouring cables) and the interaction of wind, rain and cable. In these cases the adequate 3D model of turbulent wind is highly desirable.

Obtained statistical and frequency properties of the longitudinal, lateral and vertical component of the measured turbulent wind can find a wider use in the analysis and design of structures in similar areas.

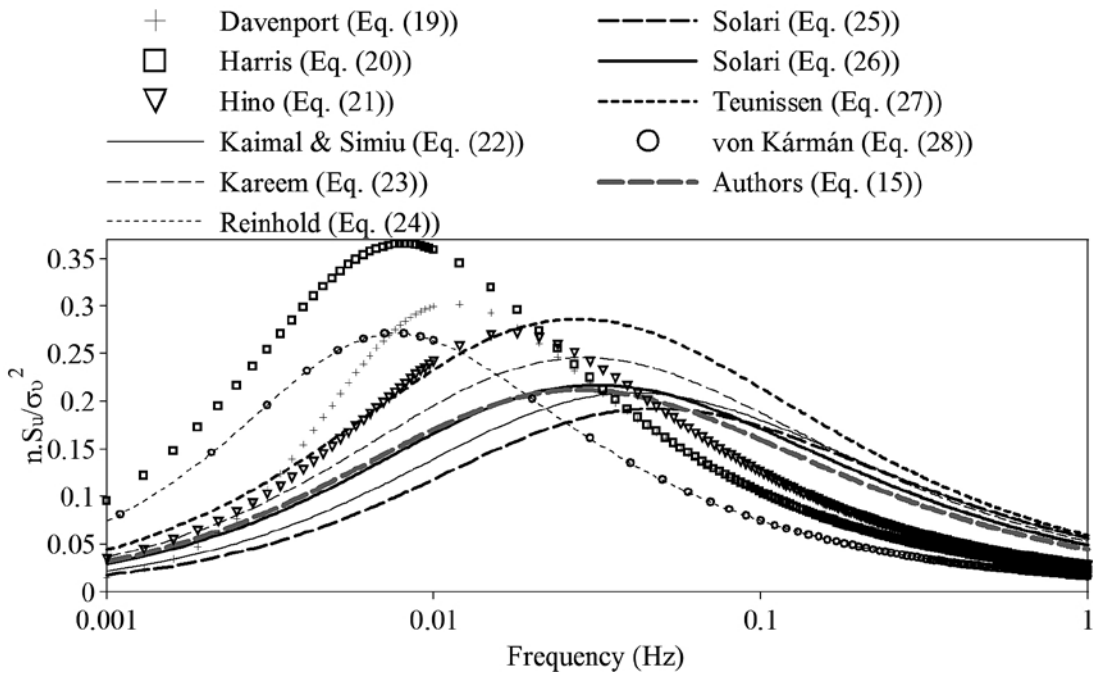


Figure 7. Comparison of the mean power spectral density function obtained from the measurement of the wind velocity component in the longitudinal direction with those obtained by analytical expressions proposed by other authors

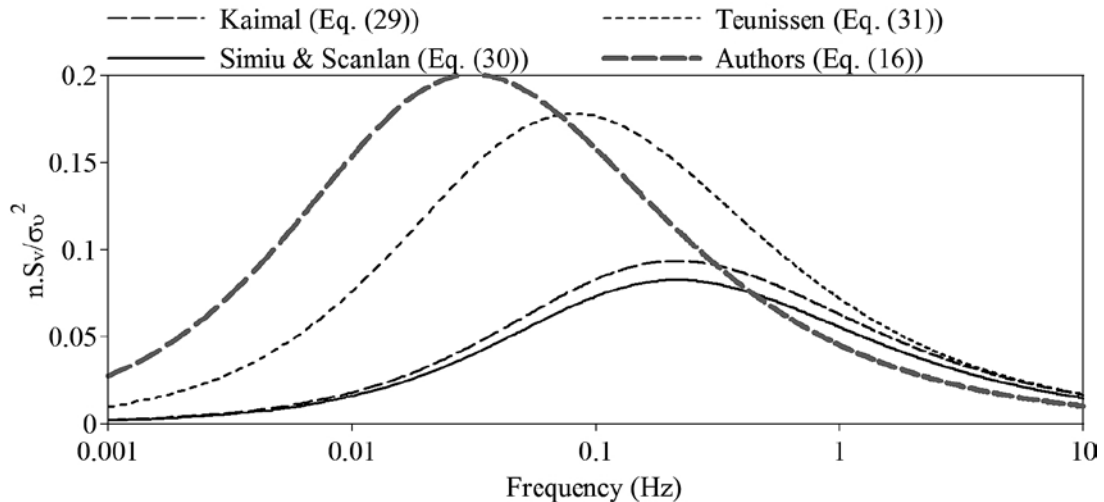


Figure 8. Comparison of the mean power spectral density function obtained from the measurement of the wind velocity component in the lateral direction with those obtained by analytical expressions proposed by other authors

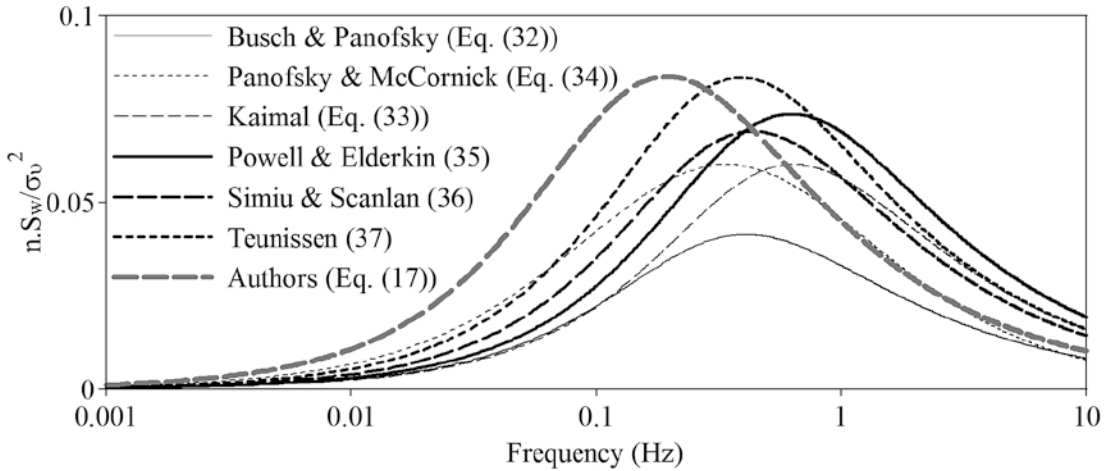


Figure 9. Comparison of the mean power spectral density function obtained from the measurement of the wind velocity component in the vertical direction with those obtained by analytical expressions proposed by other authors

## 5. Generation and numerical simulation of wind velocity histories

### 5.1 Numerical method

Shinozuka and Jan (1972) showed that the fluctuating velocity component  $u'(z, t)$  of the wind velocity  $u(z, t) = \bar{u}(z) + u'(z, t)$  at any time  $t$  can be expressed as

$$u'(z, t) = \sqrt{2} \sum_{j=1}^N \sqrt{S_u(z, n_j) \Delta n} \cos(2\pi n_j t + \phi_j) \quad (18)$$

where  $S_u(z, n_j)$  is the value of the power spectral density function for the fluctuating component of wind at the frequency  $n_j = j\Delta n$  for  $j = 1, 2, \dots, N$ ,  $\Delta n_{max}/N$ , is the frequency step where  $N$  is the number of discrete frequencies from the given spectral coordinate and  $\phi_j$  is the phase angle with a uniform probability distribution function that varies randomly between 0 and  $2\pi$ .

The technique for generating single wind histories using a Fourier series is based on the simulation of fluctuations of wind velocities  $u'(z, t)$  (for  $t = i\Delta t$  where  $i = 0, 1, \dots, k$  and  $k$  is the number of time steps), by the superposition of cosines of  $N$  each frequency step  $\Delta n$  at the each time step  $\Delta t$ .

The frequency range  $n_{max}$  in Eq. (18), which is divided into  $N$  parts, must contain all the significant natural frequencies of the structure. In the case of nonlinear structures the frequency step  $\Delta n = n_{max}/N$  needs to be small, as the natural frequencies of such structures vary with the amplitude of the response.

## 5.2 Results of simulation

The WindSimul computational software was created in the Matlab numerical computing environment to simulate the wind velocity components in all directions (MATLAB, 2006).

Power spectral density functions given by Eq. (15), (16) and (17) were used for the S1 simulation (60 s simulation) of the wind velocity component in the longitudinal, lateral and vertical direction by the developed program. The power spectral density functions proposed by Solari, 1993 (EN 1991-1-4, 2005) (Eq. (26)) in the longitudinal direction, by Simiu and Scanlan (Eq. (60)) in the lateral direction and by Simiu and Scanlan (Eq. (36)) in the vertical direction were used for the S2 simulation (60 s simulation) by the developed program.

On the basis of the random selected records from experimentally measured wind velocities with durations of 60 s, numerical simulations of the measured wind velocity component in the longitudinal, lateral and vertical direction were determined using the created program. For the best portrayal of the experimental measurements by simulations the following inputs were chosen in accordance with the measured record: the duration of the record  $t = 60$  s, the mean wind velocity component in the longitudinal direction  $\bar{u} = 9.5945 \text{ ms}^{-1}$ , in the lateral direction  $v = -0.0144 \text{ ms}^{-1}$  and in the vertical direction  $w = 2.1245 \text{ ms}^{-1}$ , an effective height above the zero level  $z = 5.0$  m, the terrain category III according to EN 1991-1-4, 2005 with the corresponding roughness length  $z_0 = 0.3$  m, the frequency of the recording 20 Hz and the frequency range from 0 to 10 Hz ( $n_{max} = 10 \text{ Hz}$ ). From these input data the number of recorded time steps  $k = 1200$  and the number of discrete frequencies  $N = 600$  were considered for the simulations. The simulation with duration of 60 s represents one period.

For the number of discrete frequencies  $N$  to be chosen with respect to zero mean velocity of the fluctuating wind component, a random function must consequently include one period. To achieve one period of the fluctuating component, the number of discrete frequencies is  $N = tn_{max}$ .

Time courses of the wind velocity components in the longitudinal, lateral and vertical direction of the randomly selected measured record with duration of 60 s and their S1 simulations are shown in Figure 10 and Figure 11.

Statistical characteristics of the measured and simulated wind velocity components in the longitudinal, lateral and vertical direction (S1 simulation) are introduced in Table 1, 2 and 3.

Relative rates and distribution functions of the occurrence of the measured (60 s record) and simulated (S1 and S2 simulations) wind velocity components in the longitudinal, lateral and vertical direction as well as their corresponding power spectral density functions are shown in Figure 12 and 13.

A comparison of the results obtained from the measured and simulated data was presented. These results confirmed the required correctness of the simulated fluctuating wind velocity histories and the possibility of their further use in dynamic analyses.

## 6. Conclusions

The results of the analyses of the in situ measured wind records with a sampling frequency of 20 Hz and with the duration of 1 year were presented. For each data set statistical characteristics and power spectral density functions of the fluctuating velocity components of measured wind in the longitudinal, lateral and vertical direction were defined.

On the basis of the experimentally measured records of turbulent wind velocities the simulations of the wind field histories in the individual directions were generated using the created Wind-

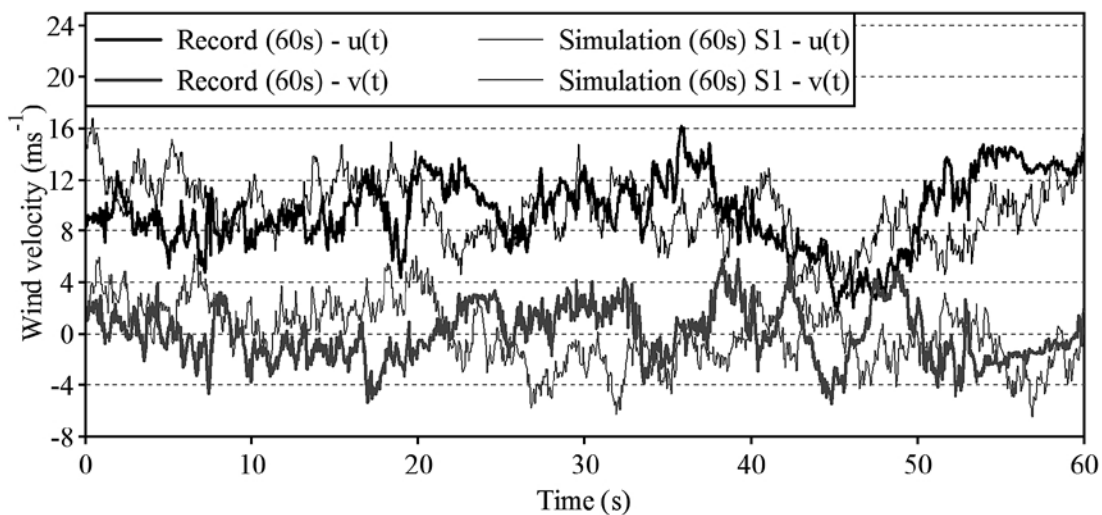


Figure 10. Time courses of the experimentally measured and simulated wind velocity components in the longitudinal  $u(t)$  and lateral direction  $v(t)$

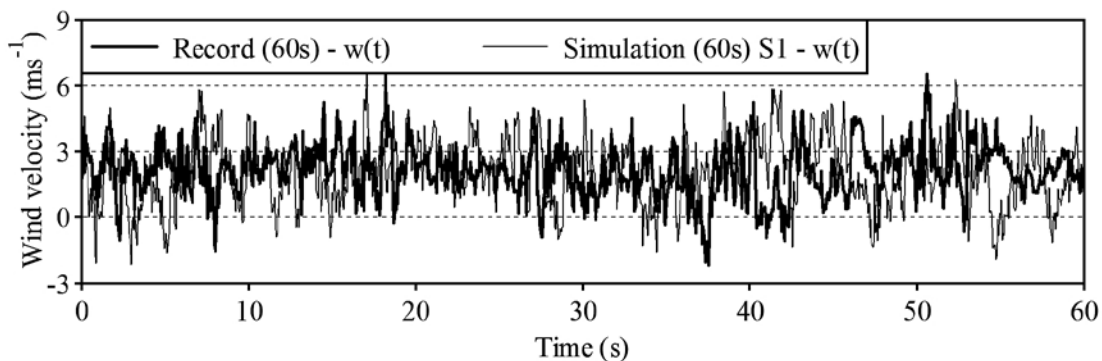
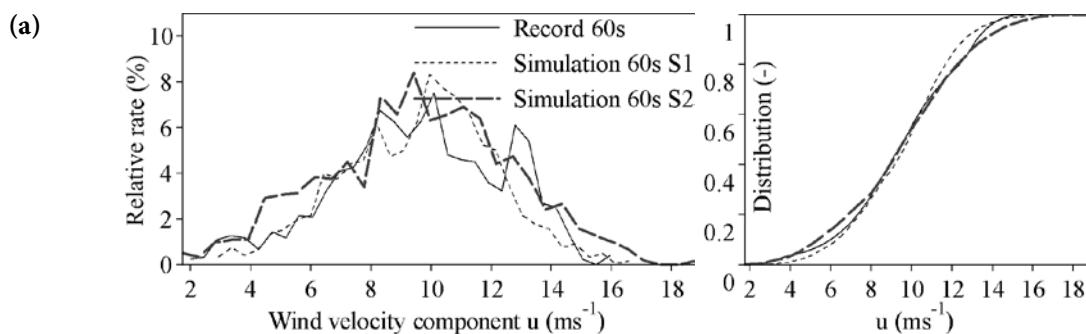


Figure 11. Time courses of the experimentally measured and simulated wind velocity component in the vertical direction  $w(t)$



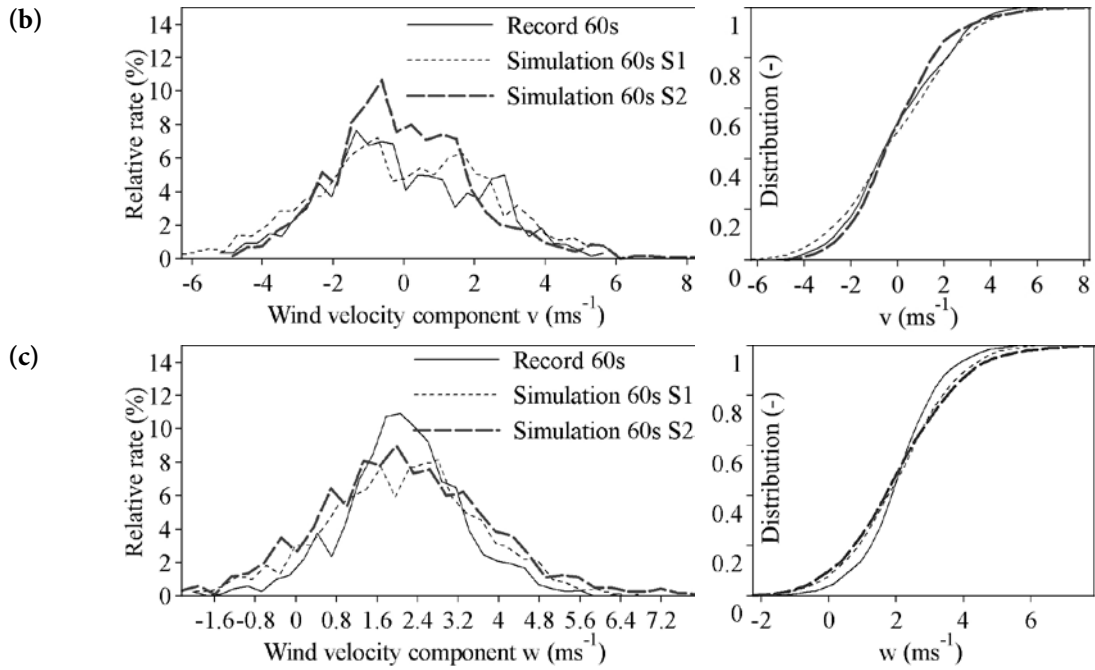
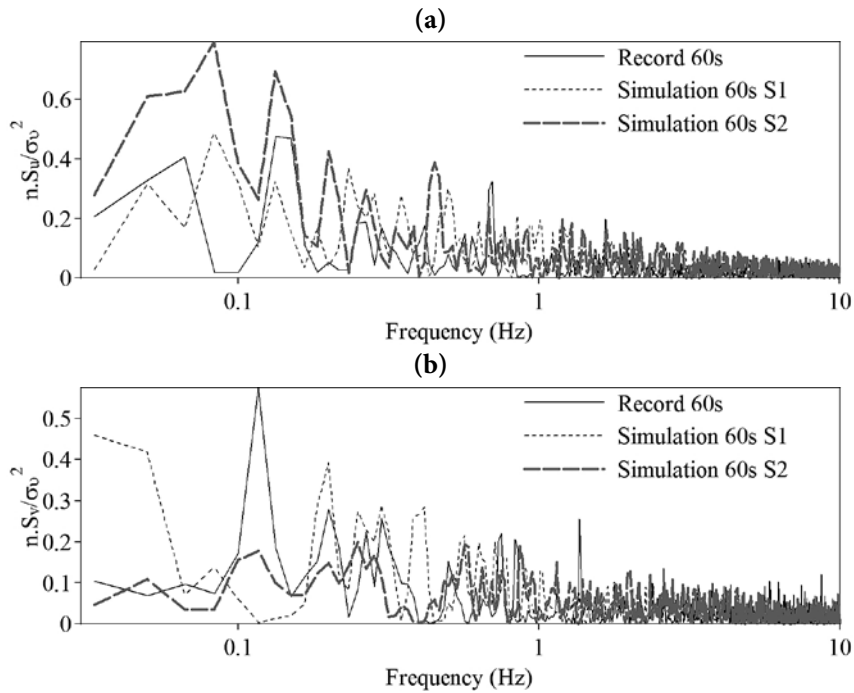


Figure 12. Comparisons of relative rates and distribution functions of the occurrence of the measured and simulated wind velocity components in the longitudinal (a), lateral (b) and vertical (c) direction



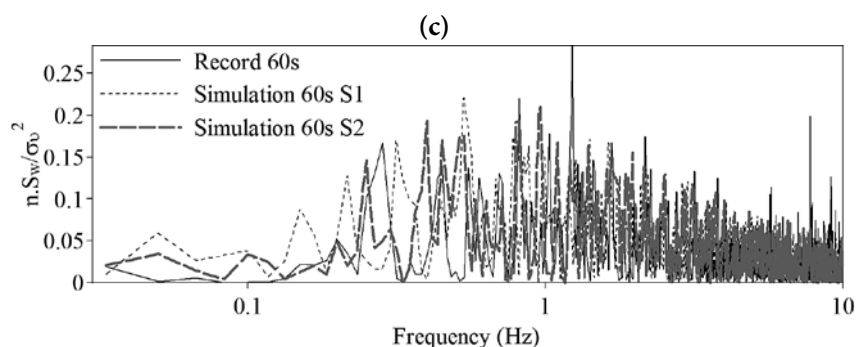


Figure 13. Comparisons of power spectral density functions of the measured and simulated wind velocity components in the longitudinal (a), lateral (b) and vertical (c) direction

Simul program and the evaluation of their statistical and frequency properties were performed. The physical importance of the mathematical approach and the functionality of the developed program were demonstrated and proved.

In the standard EN 1991-1-4, 2005 only the power spectral density function for the longitudinal direction is available. This study offers power spectral density functions of the fluctuating velocity components of measured wind for all three directions. For a detailed dynamic analysis of structures subjected to turbulent wind the spatial wind histories are required to obtain their realistic aero-elastic response and behaviour characteristics.

Obtained statistical and frequency properties of the longitudinal, lateral and vertical component of the measured turbulent wind can find a wider use in the dynamic analysis and design of structures in similar areas.

Further investigations, aimed at a deeper comprehension of the nonlinear dynamic response of wind-excited cables, should consider a fluid-solid coupled simulation of the cable interaction with the environment under the turbulent wind field and represent a future task for the authors.

### Acknowledgements

This work is part of Research Projects No. 1/0321/12 and No. APVV-0179-10, partially founded by the Scientific Grant Agency and the **Slovak Research and Development Agency** of the Ministry of Education, Science, **Research** and Sport of the Slovak Republic and the Slovak Academy of Sciences. The present research has been carried out within the project Centre of excellent integrated research for progressive building structures, materials and technologies, supported by European Union Structural funds. Special thank belongs to the staff of the Institute of Systems Biology and Ecology from the Academy of Sciences of the Czech Republic for providing the measured wind records.

### REFERENCES

- [1] Carassale L., Solari, G. (2002), "Wind modes for structural dynamics: a continuous approach", *Probabilist Eng. Mech.*, 17, 157-66.
- [2] Chen, X., Matsumoto, M., Kareem, A. (2000), "Time domain flutter and buffeting response analysis of bridges", *Journal of Engineering mechanics*, ASCE, 126, 7-16.

- [3] Davenport, A. G. (1961), "The spectrum of horizontal gustiness near the ground in high winds", *Quart. J. Royal Meteorol. Soc.*, 87, 194-211.
- [4] EN 1991-1-4 (2005), "Actions on structures, Part 1-4: General actions – Wind actions", CEN.
- [5] Fischer, O, Kolousek, V, Pirner, M., (1977), "Aeroelasticity of building structures", Academia, Prague.
- [6] FlexPro (2005), "Documentation", Version 7.0.24, Weisang GmbH, St. Ingbert, Germany.
- [7] Frichtl, G. H., McVehil, G. E., (1970), "Longitudinal and lateral spectra of turbulence in the atmospheric boundary layer at the Kennedy space center", *Journal of Applied Meteorology*, 9 (1), 51-63.
- [8] Fu, J. Y., Liang, S. G. and Li, Q. S. (2007), "Prediction of wind-induced pressures on a large gymnasium roof using artificial neural networks", *Computers and Structures*, 85 (3-4), 179-192.
- [9] Hanzlik, P., Diniz, S., Grazini, A., Grigoriu, M. and Simiu, E. (2005), "Building orientation and wind effects estimation", *Journal of Engineering Mechanics*, ASCE, 131(3), 254-258.
- [10] Harris, R. I., (1971), "The nature of wind, the modern design of wind-sensitive structures", Construction Industry Research and Information Association, London-UK.
- [11] Hino, M. (1971), "Spectrum of gusty wind", *Proceedings of the 3rd International Conference on Wind Effects on Buildings and Structures*, Tokyo, Japan, 69-77.
- [12] Hiriart, D., Ochoa, J. L. and Garcia, B. (2001), "Wind power spectrum measured at the San Pedro Martir Sierra", *Revista Mexicana de Astronomia y Astrofisica*, 37(2), 213-220.
- [13] Holmes, D. J. (2001), "Wind loading of structures", Spon Press, London – New York.
- [14] Jang, J. J., Lee, Y. L. (1998), "A study of along wind speed power spectrum for Taiwan area", *Journal of Marine Science and Technology*, 6, 71-77.
- [15] Kaimal, J. C., Wyngaard, J. C., Izumi, Y. and Cote, O. R. (1972), "Spectral characteristics of surface layer turbulence", *Quart. J. Royal Meteorol. Soc.*, 98, 563-589.
- [16] Kareem, A. (1985a), "Wind-induced response analysis of tension leg platforms", *Journal of Structural Engineering*, 111 (1), 37-55.
- [17] Kareem, A. (1985b), "Structure of wind field over the ocean", *Proceedings of the International Workshop on Offshore Winds and Icing*, Halifax, Nova Scotia, 225-235.
- [18] Kareem, A. (2008), "Numerical simulation of wind effects: A probabilistic perspective", *Journal of Wind Engineering and Industrial Aerodynamics*, 96(10-11), 1472-1497.
- [19] Lazzari, M., Saetta, A. V. and Vitaliani, R. V. (2001), "Non-linear dynamic analysis of cable-suspended structures subjected to wind actions", *Computers and Structures*, 79(9), 953-969.
- [20] Li, L. et al., (2012), "Modeling typhoon wind power spectra near sea surface based on measurements in the South China sea", *Journal of Wind Engineering and Industrial Aerodynamics*, 565-576.
- [21] Li, Q. S., Zhi, L. H. and Hu, F. (2009), "Field monitoring of boundary layer wind characteristics in urban area", *Wind and Structures, An Int'l Journal*, 12(6), 553-574.
- [22] Masters, F. J., Tieleman, H. W., Balderrama, J. A. (2010), "Surface wind measurements in three Gulf Coast hurricanes of 2005", *Journal of Wind Engineering and Industrial Aerodynamics*, 98, 533-547.
- [23] MATLAB (2006), "Documentation, Optimization Toolbox User's Guide", Version 3.1, the MathWorks, Inc., Natick, MA, USA.
- [24] Naprstek, J. (2001) "Stability domains of wind-excited random nonlinear systems through Lyapunov function", *J. Wind Eng. Ind. Aerodynam.*, 89, 1499-1512.
- [25] Olesen, H. R., Larsen, S. E., Højstrup, J., (1984), "Modelling velocity spectra in the lower part of the planetary boundary layer", *Boundary-Layer Meteorology*, 29 (3), 285-312.

- [26] Panofsky, H. A., Dutton, J. A., (1984), "Atmospheric turbulence: Models and methods for engineering applications", John Wiley & Sons, Inc. – New York.
- [27] Panofsky, H. A. and McCormick, R. A. (1960), "The spectrum of vertical velocity near the surface", *Quart. J. Royal Meteorol. Soc.*, 86, 546-564.
- [28] Powell, D. C., Elderkin, C. E. (1974), "An investigation of the application of Taylor's hypothesis to atmospheric boundary layer turbulence", *Journal of the Atmospheric Sciences*, 31, 990-1002.
- [29] Shiau, B. S., Chen, Y. B., (2002), "Observation on wind turbulence characteristics and velocity spectra near the ground at the coastal region", *Journal of Wind Engineering and Industrial Aerodynamics*, 90, 1671-1681.
- [30] Shinozuka, M. and Jan, C. M. (1972), "Digital simulation of random processes and its applications", *Journal of Sound and Vibration*, 25(1), 111-128.
- [31] Simiu, E. (1974), "Wind spectra and dynamic along-wind response", *Journal of Structural Division, ASCE*, 100(9), 1897-1910.
- [32] Simiu, E., Scanlan, R. H., (1986), "Wind Effects on Structures", 2nd Edition, John Wiley & Sons – New York.
- [33] Simiu, E., Scanlan, R. H., (1996), "Wind Effects on Structures: Fundamentals and Applications to Design", John Wiley & Sons – New York.
- [34] Solari, G. (1987), "Turbulence modelling for gust loading", *Journal of Structural Engineering, ASCE*, 113, 1550-1569.
- [35] Solari, G. (1993), "Gust buffeting I: Peak wind velocity and equivalent pressure", *Journal of Structural Engineering, ASCE*, Vol. 119, No. 2, 365-382.
- [36] Solari, G. and Piccardo, G. (2001), "Probabilistic 3-D turbulence modelling for gust buffeting of structures", *Probabilistic Engineering Mechanics*, 16, 73-86.
- [37] Tamura, Y., Kareem, A., Solari, G., Kwok, K.C.S., Holmes, J.D., (2001), "Report by working group WGE-dynamic response".
- [38] Tesar, A., Vrabec, M., Juhasova, E. (2008), "Aeroelasticity of slender bridges with wind-screen barriers", *Building Research Journal*, 56, 131-148.
- [39] Teunissen, H. W. (1980), "Structure of mean winds and turbulence in the planetary boundary layer over rural terrain", *Bound Layer Meteorol*, 19, 187-221.
- [40] Tieleman, H. W., (1995), "Universality of velocity spectra", *Journal of Wind Engineering and Industrial Aerodynamics*, 56 (1), 55-69.
- [41] Von Kármán, T., (1948), "Progress in the structural theory of turbulence", *Proceedings of the National Academy of Science, Washington, D. C.*, 194-211.
- [42] Yu, B. et al., (2008), "Hurricane wind power spectra, cospectra, and integral length scales", *Boundary-Layer Meteorology*, 129 (3), 411-130.